Effects of band division on radiative calculations

Hua Zhang
China Meteorological Administration
National Climate Center
Laboratory for Climate Studies
Beijing 100081
China
E-mail: huazhang@cma.gov.cn

Tsuneaki Suzuki
Japan Agency for Marine-Earth Science and Technology
Frontier Research Center for Global Change
Yokosuka 237-0061
Japan

Teruyuki Nakajima
University of Tokyo
Center for Climate System Research
Tokyo 113-8654
Japan

Guangyu Shi
Institute of Atmospheric Physics
State Key Laboratory of Numerical Modeling for Atmospheric Sciences and Geophysical Fluid Dynamics
Beijing 100029
China

Xiaoye Zhang
China Meteorological Administration
Chinese Academy of Meteorological Sciences
Beijing 100081
China

Yi Liu
Institute of Atmospheric Physics
Laboratory for Middle Atmosphere and Global Environment Observation
Beijing 100029
China

Abstract. Band division is an important basis in radiative calculations, and the configuration of band divisions for various research purposes directly influences the accuracy and speed of radiative transfer computations. We explore four band-division schemes and their impacts on computed radiative fluxes and cooling rates. We explain that discrepancies in solar radiation at the surface that exist between radiation models and observations under clear-sky conditions arise partly from ignoring minor gases and weak absorption bands for major gases. [DOI: 10.1117/1.2160521]

Subject terms: band division; radiative calculation; line by line; correlated *k*-distribution.

Paper 050004RR received Jan. 4, 2005; revised manuscript received Jun. 9, 2005; accepted for publication Jun. 11, 2005; published online Jan. 24, 2006.

1 Introduction

Radiation is one of the most important factors controlling climate simulations. Climate is sensitive to external radiative forcing, and longwave radiation influences weather and climate. A minor error in the calculation of shortwave heating rates can introduce a significant deviation in climate modeling because solar radiation is the ultimate source of nearly all energy on earth. Recent computer advances have enabled the use of radiative transfer algorithms that are more accurate.

0091-3286/2006/$22.00

General circulation models (GCMs) before 1985 considered only a few major IR absorptive bands, such as CO_2 15 μm, H_2O 6.3 m, and O_3 9.6 μm, because of limitations in both computer power and knowledge of the radiative effects of other greenhouse gases. Research focused on parameterizing the effects of these absorptive gases (see, e.g., Refs. 1–3). However, it is well known[4,5] that opaqueness due to CH_4 and N_2O in the IR, primarily between 1200 and 1400 cm^{-1}, strongly influences the longwave radiative balance of the earth's surface-troposphere system. The effects of CH_4 and N_2O in previous GCMs have either been ignored or simulated with an effective amount of CO_2 (Refs. 6 and 7). Nevertheless, researchers found substantial

differences in the tropospheric response to radiative perturbations when effective amounts of CO_2were used.[8,9] Subsequently, N_2O and CH_4 have been treated individually in GCMs. Past studies[10–16] have also developed parameterizations for the absorption of solar radiation by H_2O, CO_2, O_3, and O_2. Some of those parameterizations include the O_2-A (0.762 m) and O_2-B (0.688 m) bands, and some do not. The absorption by oxygen in these bands is very weak, but it contributes significantly to the solar energy budget of the atmosphere because of the large amount of O_2 in the atmosphere and because the bands are near the peak in incoming solar radiation.

Peixoto and Oort[17] show blackbody curves for solar and terrestrial radiation. The curves show that gases absorb with different strengths at different wavelengths. Cases near the surface differ from cases at 11 km, reflecting the different distributions of gas with height. How to divide the band is an important practical problem in radiative transfer calculations that include these absorptive spectra, their strengths, overlapping bands, and concentration distributions with height. Furthermore, the calculations must consider the wavelength dependence of the solar source in addition to changes in the Planck function driven by changes in thermal radiation. Band division influences calculation speed and accuracy, and it is difficult to design one scheme that is applicable for various research purposes. A substantial part of the computation time in GCMs is devoted to radiative transfer calculations[18,19] and the desire to speed calculations in GCMs typically results in the adoption of a relatively coarse scheme of band division that ignores weak absorption by major gases and most absorption by minor gases. However, chemical models require more precise radiative transfer calculations, so an accurate band-dividing scheme that includes minor absorptions must be included. This paper develops five different schemes to address different research goals and compares the radiative flux and cooling rate results for the schemes with the most accurate reference. Radiative forcing is also computed for the ignored gas absorption at every band-dividing scheme under clear-sky conditions.

The algorithm is described in Sec. 2. Section 3 describes results from the different schemes for the radiative flux and cooling rate. Section 4 presents the conclusion.

2 Algorithm

The line-by-line radiative transfer model (LBLRTM)[20,21] is used to calculate the line absorption coefficients of absorptive gases, including H_2O, CO_2, O_3, N_2O, CH_4, and O_2, and the continuum absorption coefficients of H_2O, CO_2, O_3, and O_2. The radiative transfer algorithm developed by Zhang et al.[22] is reviewed here briefly. Longwave radiative transfer for homogeneous parallel sublayers of a planetary atmosphere is calculated assuming thermal radiation from an isolated layer, as described in Lacis and Oinas.[23] Flux transmittance is computed using a modified diffusion factor.[24] In an inhomogeneous atmosphere, the vertical layers can be expressed as many homogeneous sublayers. The upward and downward radiative flux is then calculated layer by layer. Shortwave radiative transfer is described in Nakajima et al.[25] Here, only atmospheric absorption is considered for the overall calculation.

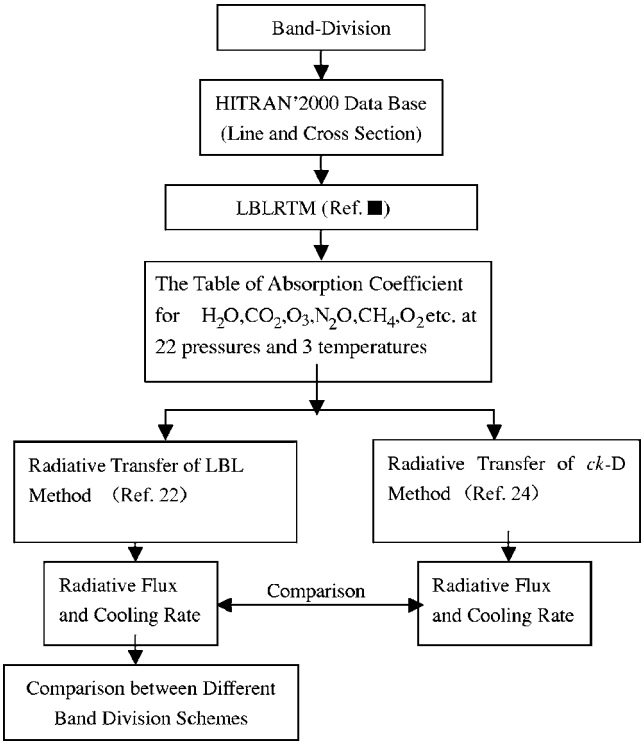

Fig. 1 Schematic of the algorithm.

Figure 1 shows a schematic of the algorithm. The updated line database from[26] HITRAN 2000 is used as the initial input for LBLRTM to calculate a table of line and continuum absorption coefficients at 22 pressures and 3 temperatures. The 22 pressures are 0.01, 0.0158, 0.0215, 0.0251, 0.0464, 0.1, 0.158, 0.215, 0.398, 0.464, 1.0, 2.15, 4.64, 10.0, 21.5, 46.4, 100.0, 220.0, 340.0, 460.0, 700.0, and 1080.00 hPa, and are from the midlatitude summer atmosphere provided by the Air Force Geophysics Lab (AFGL). The three temperatures are 160, 260, and 340 K, and they cover the range of temperatures in the earth atmosphere. Finally, line-by-line (LBL) integrations and correlated *k*-distribution (*ck*-D) methods are used to calculate the radiative fluxes and cooling rates. See Refs. 22 and 27 for details. The atmosphere is divided into 75 layers for this calculation, and the vertical resolution is 1 km. Surface height is 0 km, and the top of atmosphere (TOA) for the calculation is 0.1 hPa. The number of *k*-intervals is fixed at 16 for every band in all schemes for convenience in the comparisons made here. Data from the U.S. standard atmosphere[28] (USS, for short) are used for most of the calculations. The surface albedo is set to 0.2 and the solar zenith angle is 60 deg for the solar calculations.

3 Effects of Various Band-Division Schemes on Radiative Flux and Cooling Rate

Table 1 presents four band-division schemes, including 17 bands with 8 in the longwave region and 9 in the shortwave region, 21 bands (11 longwave, 10 shortwave), 27 bands (14 longwave, 13 shortwave), and 55 bands (24 longwave, 31 shortwave). The wavelengths and types of absorptive gases involved in every band are listed for each scheme following data on blackbody radiation and atmospheric ab-

Table 1 Band configurations.

N	17-band (cm^{-1})	Gas	21-band (cm^{-1})	Gas	27-band (cm^{-1})	Gas	55-band (cm^{-1})	Gas
1	10	H_2O	10	H_2O	10	H_2O	10	H_2O
2	250	H_2O	250	H_2O	250	H_2O	50	H_2O
3	550	H_2O,CO_2	430	H_2O	430	H_2O	60	H_2O
4	780	H_2O	530	H_2O, CO_2, N_2O	530	H_2O, CO_2, N_2O	80	H_2O
5	990	H_2O, O_3	630	H_2O, CO_2, O_3	630	H_2O,CO_2, O_3	100	H_2O
6	1,200	H_2O, N_2O, CH_4	700	H_2O, CO_2, O_3	700	H_2O, CO_2, O_3	120	H_2O
7	1,430	H_2O	820	H_2O	820	H_2O	160	H_2O
8	2,110	H_2O,CO_2, N_2O	940	H_2O, CO_2, O_3	940	H_2O, CO_2, O_3	220	H_2O
9	2,680	H_2O	1,200	H_2O, N_2O, CH_4	1,200	H_2O, CH_4	280	H_2O
10	5,200	H_2O	1,430	H_2O	1,300	H_2O, N_2O, CH_4	350	H_2O
11	12,000	H_2O, O_3	2,110	H_2O, CO_2, N_2O	1,390	H_2O	430	H_2O
12	22,000	—	2,680	H_2O, CO_2, CH_4	1,480	H_2O	530	H_2O, CO_2, N_2O
13	31,000	O_3	4,540	H_2O, CO_2	1,810	H_2O	630	H_2O, CO_2, O_3
14	33,000	O_3	6,150	H_2O	2,110	H_2O, CO_2, N_2O	700	H_2O, CO_2, O_3
15	35,000	O_3	12,000	H_2O, O_3	2,680	H_2O, CH_4	820	H_2O
16	37,000	O_3, O_2	22,000	—	3,500	H_2O, CO_2	940	H_2O, CO_2, O_3
17	43,000	O_3, O_2	31,000	O_3	3,900	H_2O, CH_4	1,110	H_2O, CO_2, O_3
18	49,000		33,000	O_3	4,540	H_2O	1,200	H_2O, N_2O, CH_4
19			35,000	O_3	6,150	H_2O	1,350	H_2O, CH_4
20			37,000	O_3, O_2	8,050	H_2O	1,430	H_2O
21			43,000	O_3, O_2	12,000	H_2O, O_3	1,600	H_2O
22			49,000		22,000	—	1,810	H_2O, CO_2, O_3
23					31,000	O_3	2,110	H_2O, CO_2, N_2O
24					33,000	O_3	2,380	CO_2, N_2O
25					35,000	O_3	2,680	H_2O, CH_4
26					37,000	O_3, O_2	3,080	H_2O, N_2O
27					43,000	O_3, O_2	3,400	H_2O, CO_2
28					49,000		3,890	H_2O, CH_4
29							4,540	H_2O, CO_2
30							5,400	H_2O
31							6,150	H_2O, CO_2
32							7,600	H_2O, O_2

Table 1 (*Continued.*)

N	17-band (cm^{-1})	Gas	21-band (cm^{-1})	Gas	27-band (cm^{-1})	Gas	55-band (cm^{-1})	Gas
33							8,050	H_2O
34							10,000	H_2O
35							12,000	O_3, O_2
36							13,200	H_2O, O_3
37							14,500	H_2O, O_3
38							16,000	H_2O, O_3
39							18,000	H_2O, O_3
40							20,000	O_3
41							22,000	—
42							29,000	O_3
43							31,000	O_3
44							33,000	O_3
45							35,000	O_3
46							37,000	O_3, O_2
47							39,000	O_3,O_2
48							41,000	O_3, O_2
49							43,000	O_3, O_2
50							45,000	O_3, O_2
51							47,000	O_3, O_2
52							49,000	O_3, O_2
53							51,000	O_3, O_2
54							53,000	O_3, O_2
55							55,000	O_2
							57,000	

sorption in Peixoto and Oort[17] and Goody and Young.[29] The scheme with only 17 bands includes five major gases and their main absorption bands in the long wave and IR. The method with 21 bands includes more absorption by those five gases and absorption by CH_4 in the 1200 to 1430-cm^{-1} region; the 27-band scheme includes much more absorption than the 21-band scheme, such as CH_4 absorption in the IR. The most accurate band division scheme is the 55-band scheme, which includes the O_2-A and O_2-B bands and the weak bands of CO_2, N_2O, and CH_4 in the longwave and shortwave regions.

A 998-band scheme is designed and provides the most accurate reference based on the absorption spectrum in Peixoto and Oort.[17] The scheme characteristics follow. The longwave region from 10 to 2680 cm^{-1} is divided into 534 regularly spaced narrow bands that have an average interval of about 5 cm^{-1}. The shortwave region from 2680 to 50,000 cm^{-1} is divided into 464 narrow bands with an average interval of about 0.0076 μm. Each narrow band contains as many absorptive gases as possible, based on the blackbody curves in Peixoto and Oort[17] and Goody and Yung,[29] including the very weak band for the entire spectrum. The radiative fluxes and cooling rates from this 998-band scheme using LBL are the most accurate, so the ra-

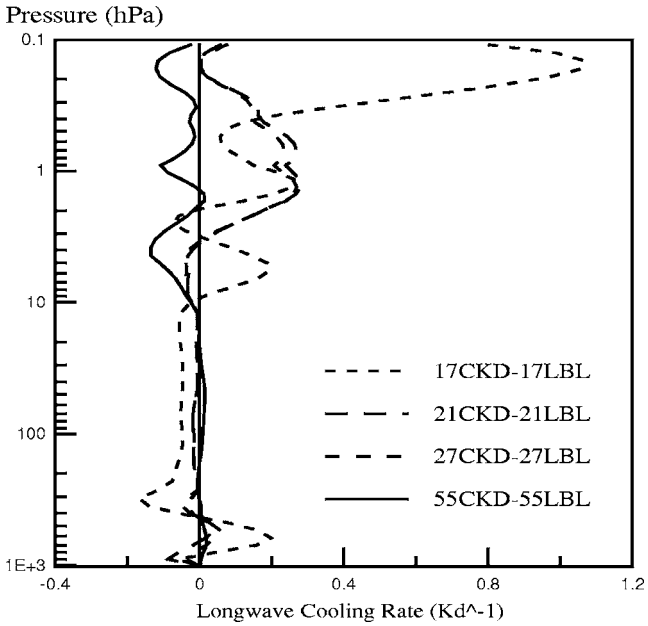

Fig. 2 Differences of longwave cooling rates between the *ck*-D and LBL method for different band-division schemes. CKD in the figure represents *ck*-D method.

diative flux and cooling rate results of each of the four schemes are compared with the 998-band scheme. Such comparisons will clarify the differences between the radiative schemes, revealing which are appropriate for climate models or other research purposes and which is most accurate. The comparison will also quantify the radiative forcing caused by the minor gases and weak bands that the schemes ignore.

Figure 2 shows the absolute error in the longwave cooling rates computed using the LBL and *ck*-D methods for each of the four schemes using USS, highlighting the differences between the two methods. The 17-band scheme shows the largest differences between the two methods. The more approximate results of the *ck*-D method approach the LBL results as the bands become more finely divided. The 55-band scheme in Table 1 supports accurate radiative transfer calculations for atmospheric chemical models. Similarly, the 17-band scheme that is appropriate for present climate models can be replaced by a 21- or 27-band scheme in future climate models, as computer resources become available. Table 1 is taken as a basis for the following discussion.

Figure 3 shows the differences in longwave cooling and solar heating rates calculated using the LBL method for the 17-, 21-, 27-, 55-, and 998-band schemes. In general, the differences are largest between the 17- and 998-band schemes for both longwave and shortwave radiation. However, the accuracy (about 0.02 K d^{-1}) is similar among the 17-, 21-, 27-, and 55-band schemes in the longwave region below 30 km. Errors in the 17-band scheme increase above 30 km, reaching a maximum of 0.44 K d^{-1} at 50 km. Even so, the relative error there is only 3.5%. The maximum error for shortwave heating rates in the troposphere is -0.15 K d^{-1}. An error of -1.25 K d^{-1} occurred at the TOA for the 17-band scheme. The errors in the 21- and 27-band schemes are similar and are less than 0.17 K d^{-1} in the troposphere and lower stratosphere. The 55-band approach has an accuracy of 0.08 K d^{-1} and has the smallest error relative to the reference below 50 km. Differences among schemes are mainly caused by the band-dividing configuration and error cancellation in the calculations. The number of absorptive gases considered increases with the number of band divisions. For example, the 17-band scheme neglects all absorption by minor gases and many weak bands by major greenhouse gases to satisfy the computational speed requirements for climate models.

Differences between the upward and downward longwave and shortwave fluxes from each of the four schemes and the 998-band scheme are computed using the LBL method to highlight radiative flux differences between the band division schemes. Figures 4 and 5 show the results. The 17-band scheme has the worst accuracy and the 55-band scheme has the best, except for the upward longwave flux [see Fig. 1(b)]. The maximum error in the upward longwave flux is less than 1.33 W m^{-2} for the 17-, 21-, 27-, and 55-band schemes, as shown in Fig. 4(b), and this error occurs above 32 km for each scheme. The maximum relative error is 0.5%. The maximum error for the downward longwave flux is less than 1.0 W m^{-2} for all schemes, with a maximum relative error of 0.27%, as shown in Fig. 4(d). The absolute and relative accuracies of the four schemes for the upward solar flux are 4.0, 3.3, 3.8, and 2.8 W m^{-2} and 3.4, 2.8, 3.3, and 1.7%, respectively [see Fig. 5(b)]. The absolute and relative errors for the downward solar flux are 16.0, 13.0, 15.0, and 10.0 W m^{-2} and 2.9, 2.4, 2.7, and 1.8%, respectively [see Fig. 5(d)].

The net radiative flux is defined as the upward flux minus the downward flux. Here, the upward flux is defined as positive, and a downward flux as negative. The differences in the net radiative flux at the tropopause between each of the four schemes and the 998-band scheme reflect the influence on the radiative forcing of ignoring minor gases and weak bands of major gases. Table 2 lists these differences at the TOA, tropopause, and surface. Radiative forcing associated with the ignored absorption is a maximum in the 17-band scheme, with longwave and shortwave values of 1.51 and -6.49 W m^{-2}, respectively. The differences at the surface exceed those in the tropopause in the solar region, reaching -12.54 W m^{-2} for the 17-band case. Recall that the 17-band division scheme is typical of radiation schemes in most GCMs (see, e.g., Refs. 11, 14, 25, 30, and 31). The results from the 17-band scheme suggest that ignored minor gases and weak bands can absorb an extra 3.58, 6.49, and 12.54 W m^{-2} of solar radiation arriving at the TOA, tropopause, and surface, respectively.

Li[32] noted that the surface fluxes computed by radiation models are usually larger than ground-based observations and satellite-based estimates. Discrepancies between satellite-based estimations and model simulations are of the order of 20 to 25 W m^{-2} for all sky conditions, which is comparable to the differences between model simulations and surface observations. Li maintained that two critical issues had to be addressed. First, gaps in the knowledge of the partitioning of solar energy between the atmosphere and surface must be filled. Second, the discrepancy between models and observations must be explained. This study explains part of the discrepancy: the above calculated

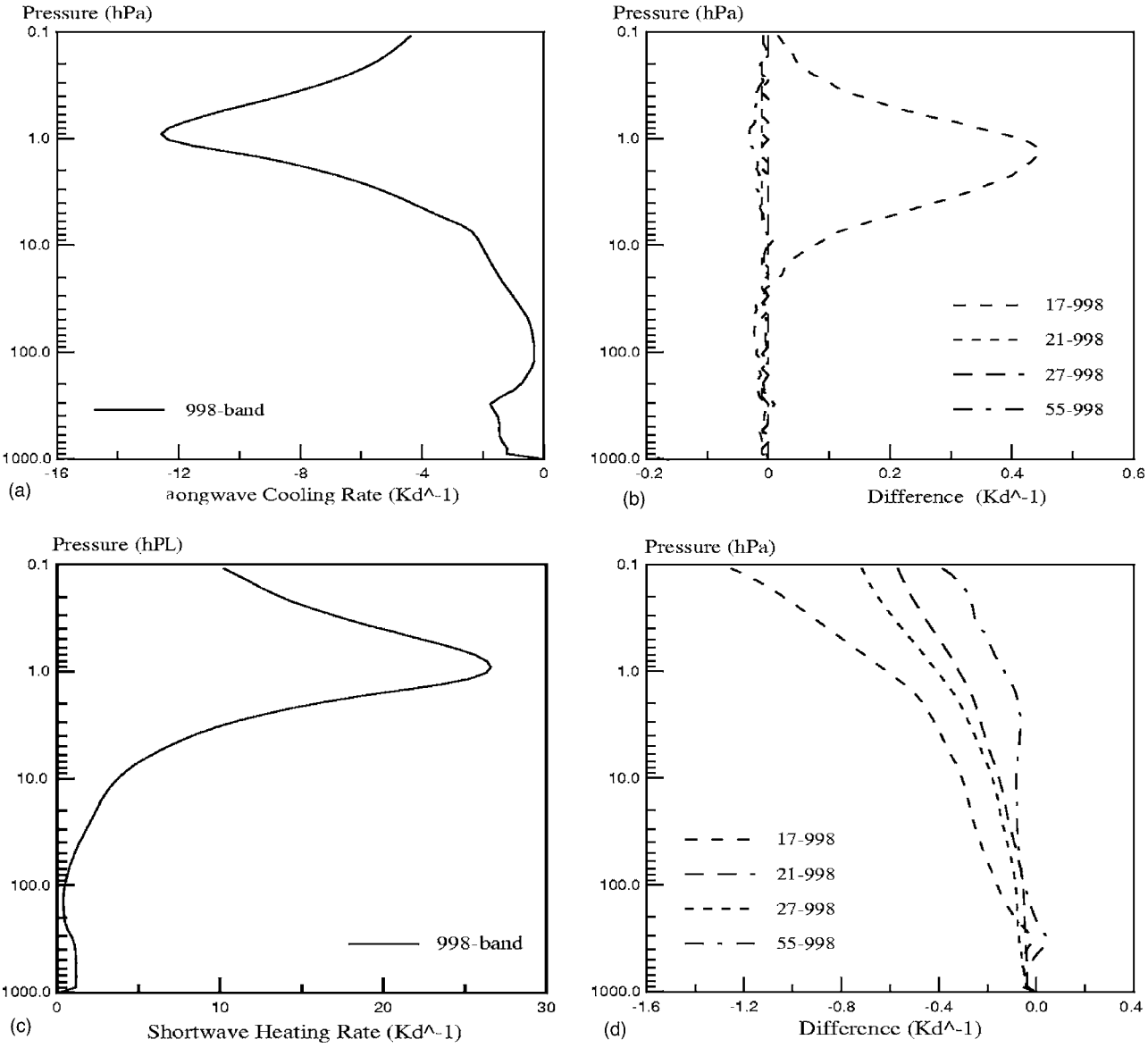

Fig. 3 Differences of longwave and shortwave heating rate between each of 4 schemes of 17-, 21-, 27-, and 55-band and the most accurate reference of 998-band scheme for USS atmosphere, where (a) and (c) stand for the most accurate reference from 998-band by LBL method and (b) and (d) are the differences for longwave and shortwave regions, respectively.

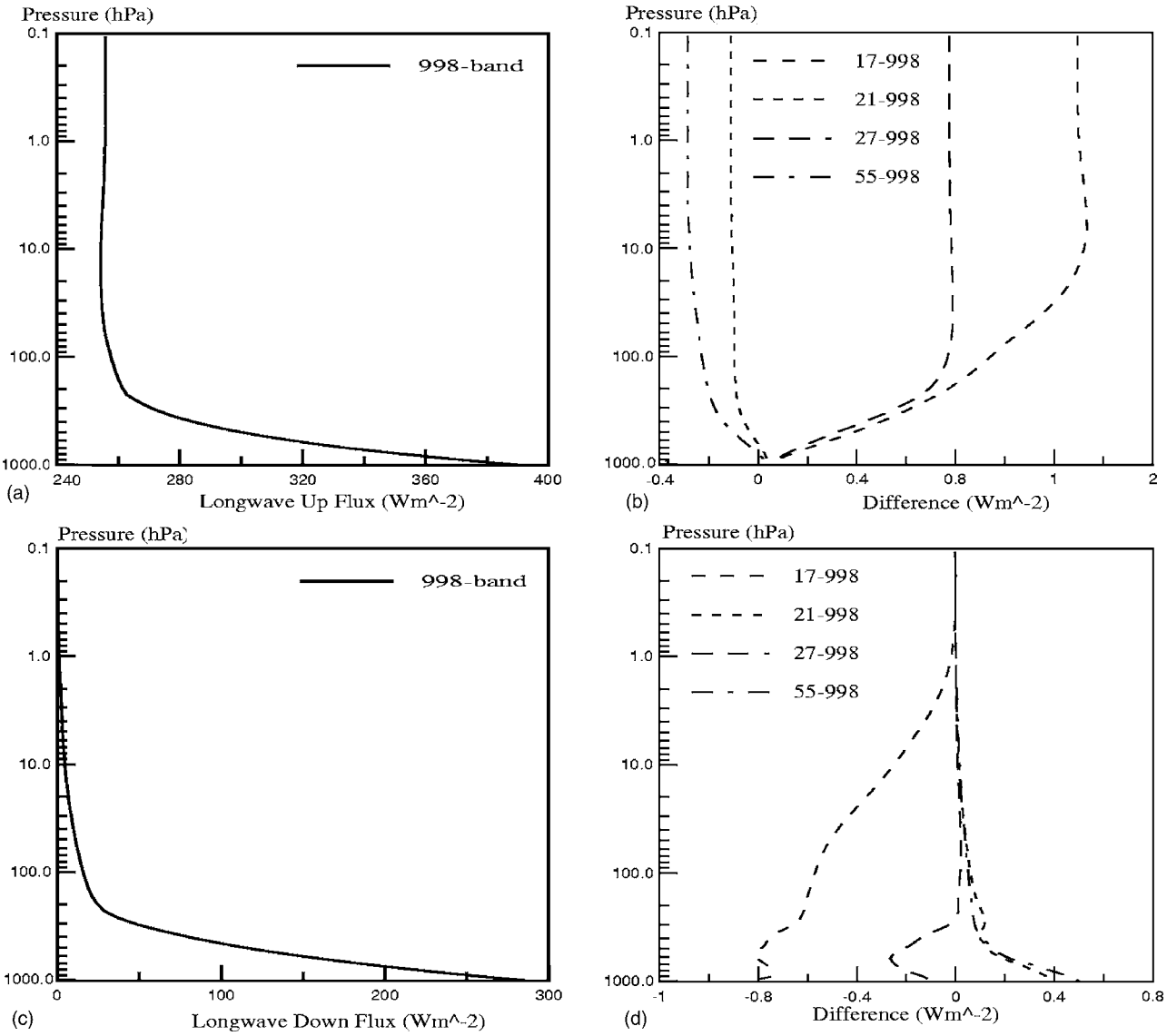

Fig. 4 Differences of longwave up and down flux between each of four schemes of 17-, 21-, 27-, and 55-band and the 998-band scheme for USS atmosphere, where (a) and (c) stand for the most accurate references from 998-band by LBL for up and down fluxes, respectively, while (b) and (d) are the differences.

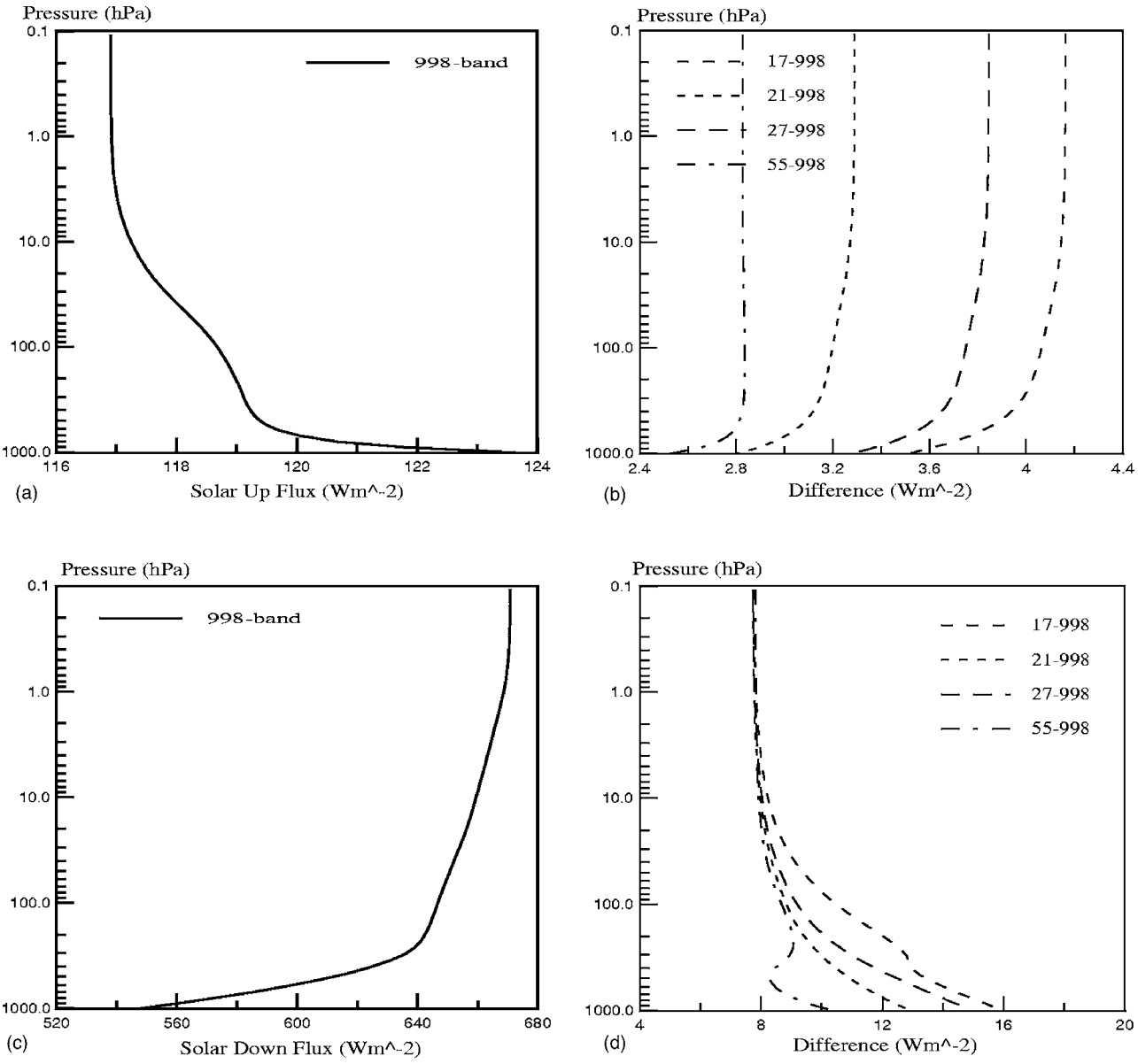

Fig. 5 Same as Fig. 4, but for the solar region.

Table 2 The difference of net flux between each of the 17-, 21-, 27-, and 55-band schemes and the 998-band scheme at the TOA, tropopause, and the surface in longwave and shortwave regions.

Region	Band Scheme	TOA ($W\,m^{-2}$)	Net Flux Tropopause ($W\,m^{-2}$)	Surface ($W\,m^{-2}$)
	998	255.57	241.79	104.85
	55-998	0.27	0.28	0.47
Long wave	27-998	0.78	0.75	0.12
	21-998	0.11	0.16	0.33
	17-998	1.30	1.51	0.88
	998	−553.98	−527.89	−422.90
	55-998	−4.98	−5.86	−7.93
Short wave	27-998	−3.85	−5.47	−11.76
	21-998	−4.44	−5.66	−10.18
	17-998	−3.58	−6.49	−12.54

12.54 $W\,m^{-2}$ for clear sky is about half of the lost absorption of 20 to 25 $W\,m^{-2}$. The observed discrepancy in the solar surface flux that exists between models and observations under clear-sky conditions[33,34] arises in part from ignoring absorption by minor gases and weak absorption by major gases, but not water vapor absorption.[35] Ignored absorption in the radiative schemes used in most GCMs is the major reason for the underestimated atmospheric absorption in the surface-troposphere system. Other lost absorption may result from absorbing aerosols.[36]

Differences in the net flux at the surface, tropopause, and TOA may be large enough to affect the radiative balance of the earth's surface atmosphere. They should be considered when exploring energy balance at the surface of the Earth.

4 Conclusion

This paper discussed the impact of various band-dividing schemes on radiative flux and cooling rate computations in both the longwave and shortwave regions for clear-sky conditions. LBL calculations show that the maximum error in the tropospheric longwave cooling rate for the 17-, 21-, 27-, and 55-band schemes is 0.02 $K\,d^{-1}$, and it is −0.17 $K\,d^{-1}$ in the shortwave region. Above the troposphere, the maximum longwave and shortwave errors are 0.44 and −1.25 $K\,d^{-1}$, respectively. The total maximum relative error for the upward and downward longwave or shortwave radiative flux for the four schemes does not exceed 3.4%.

Differences also arise between *ck*-D and LBL methods. The magnitude of errors depends on the band division. As the number of band divisions increase, the more approximate results of the *ck*-D method approach those of LBL. Numerical net flux computations show that the radiative forcings associated with ignored gas absorption in the four schemes are large. Those forcings must be considered in terrestrial energy balance studies. The absorption ignored in radiation schemes used by most GCMs is a major cause of the underestimates of atmospheric absorption in the surface-troposphere system. This partly explains why there is a discrepancy between GCM results and observations of solar radiation at the surface under clear-sky conditions.

Finally, note that all five band-dividing schemes discussed in this paper are adopted by OpenCLASTR (Open Clustered Libraries for Atmospheric Science and Transfer of Radiation) of Tokyo University of Japan for various kinds of purposes for research (http://www.ccsr.u-tokyo.ac.jp/~clastr/index.html).

Acknowledgments

This work is supported by the Aerosol Project of China Meteorological Administration, the National Natural Science Foundation of China (NSFC) (Contracts No. 40475034 and No. 40475015), and the Opening Foundation by Environmental Spectroscopy Laboratory & Atmospheric Optics Key Laboratory, Anhui Institute of Optics & Fine Mechanics, Chinese Academy of Sciences.

References

1. W.-C. Wang and P. Barry Ryan, "Overlapping effect of atmospheric H_2O, CO_2, and O_3 on the CO_2 radiative effect," *Tellus, Ser. B* **35B**, 81–91 (1983).
2. J. T. Kiehl and V. Ramanathan, "CO_2 radiative parameterization used in climate models: comparison with narrow band models and with laboratory data," *J. Geophys. Res.* **88**(9), 5191–5202 (1983).
3. S.-C. S. Ou and K.-N. Liou, "Parameterization of carbon dioxide 15 μm band absorption and emission," *J. Geophys. Res.* **88**(9), 5203–5207 (1983).
4. J. T. Houghton, G. J. Jenkins, and J. J. Ephraums, Eds., *IPCC, Climate Change: The IPCC Scientific Assessment*, Cambridge Univ. Press, New York (1990).
5. V. Ramanathan et al., "Climate-chemical interactions and effects of changing atmospheric trace gases," *Rev. Geophys.* **25**, 1441–1482 (1987).
6. V. Ramaswamy, O. Boucher, J. Haigh, D. Hauglustaine, J. Haywood, G. Myhre, T. Nakajima, G.-Y. Shi, and S. Solomon, "Radiative forcing of climate change," "Third Assessment Report—Climate Change 2001," p. 357, IPCC/WMO/UNEP (2001).
7. M. Daniel Schwarzkopf and V. Ramaswamy, "Raciative effects of CH_4, N_2O, halocarbons and the foreign-broadened H_2O continuum: a GCM experiment," *J. Geophys. Res.* **104**(D8), 9467–9488 (1999).
8. W.-C. Wang and G.-Y. Shi, "Incorporation of the thermal radiative

effect of CH_4, N_2O, CF_2C_{12}, and CFC_{13} into National Center for Atmospheric Research Community Climate Model," *J. Geophys. Res.* **96**(D5), 9097–9103 (1991).
9. S. A. Clough and M. J. Iacono, "Line-by-line calculation of atmospheric fluxes and cooling rates 2. Application to carbon dioxide, ozone, methane, nitrous oxide and the halocarbons," *J. Geophys. Res.* **100**, 16519–16535 (1995).
10. J. T. Kiehl and T. Yamanouchi, "A parameterization for absorption due to the A, B, and γ oxygen bands," *Tellus, Ser. B* **37B**, 1–6 (1985).
11. M.-D. Chou, "Parameterizations for the absorption of solar radiation by O_2 and CO_2 with application to climate studies," *J. Clim.* **3**, 209–217 (1990).
12. M.-D. Chou, "A solar radiation model for use in climate studies," *J. Atmos. Sci.* **49**, 762–772 (1992).
13. M.-D. Chou and K.-T. Lee, "Parameterizations for the absorption of solar radiation by water vapor and ozone," *J. Atmos. Sci.* **53**, 1203–1208 (1996).
14. S. M. Freidenreich and V. Ramaswamy, "A new multiple-band solar radiative parameterization for general circulation models," *J. Geophys. Res.* **104**(D24), 31389–31409 (1999).
15. M.-D. Chou, "Atmospheric solar heating in minor absorption bands," *TAO* **10**, 511–528 (1999).
16. T. A. Tarasova and B. Fomin, "Solar radiation absorption due to water vapor: advanced broadband parameterizations," *J. Appl. Meteorol.* **39**, 1947–1951 (2000).
17. J. P. Peixoto and A. H. Oort, *Physics of Climate*, p. 520, American Institute of Physics, New York (1992).
18. S. Cusack and J. M. Edwards, "Investigation k distribution methods for parameterizing gaseous absorption in the Hadley Centre Climate Model," *J. Geophys. Res.* **104**(D2), 2051–2057 (1999).
19. M.-D. Chou, X.-Z. Liang, and M. M.-H. Yan, "A thermal infrared radiation parameterization for atmospheric studies," Technical Report Series on Global Modeling and Data Assimilation, NASA/TM-2001-104606, Vol. 19, p. 1, Goddard Space Flight Center, Greenbelt, MD (2003).
20. S. A. Clough, M. J. Iacono, and J.-L. Moncet, "Line-by-line calculation of atmospheric fluxes and cooling rates: application to water vapor," *J. Geophys. Res.* **97**, 15761–15785 (1992).
21. S. A. Clough and M. J. Iacono, "Line-by-line calculation of atmospheric fluxes and cooling rates 2. Application to carbon dioxide, ozone, methane, nitrous oxide and the halocarbons," *J. Geophys. Res.* **100**, 16519–16535 (1995).
22. H. Zhang and G.-Y. Shi, "A comparison study between the two line-by-line integration algorithms," *Chin. Atmos. Sci.* **29**, 581–594 (2005).
23. A. A. Lacis and V. Oinas, "A description of the correlated k distribution method for modeling nongray gaseous absorption, thermal emission, and multiple scattering in vertically inhomogeneous atmospheres," *J. Geophys. Res.* **96**, 9027–9063 (1991).
24. H. Zhang and G.-Y. Shi, "An improved approach to diffuse radiation," *J. Quant. Spectrosc. Radiat. Transf.* **70**, 367–372 (2001).
25. T. Nakajima, M. Tsukamoto, Y. Tsushima, A. Numaguti, and T. Kimura, "Modeling of the radiative process in an atmospheric general circulation mode," *Appl. Opt.* **39**, 4869–4878 (2000).
26. L. S. Rothman and Coauthors, "The HITRAN molecular spectroscopic database and HAWKS (HITRAN Atmospheric Workstation)," http://www.hitran.com/, updated HITRAN' 2000.
27. H. Zhang, T. Nakajima, G.-Y. Shi, T. Suzuki, and R. Imasu, "An optimal approach to overlapping bands with correlated *k*-distribution method and its application to radiative calculations," *J. Geophys. Res.* **108**(D20), 4641 (2003).
28. G. P. Anderson, S. A. Clough, F. X. Kneizys, J. H. Chetwood, and E. P. Shettle, "AFGL atmospheric constituent profiles (0–120 km)," AFGL Tech. Rep., AFGL-TR-0110, Air Force Geophys. Lab., Bedford, MA (1986).
29. R. M. Goody and Y. L. Yung, *Atmospheric Radiation: Theoretical Basis*, Oxford University Press, Oxford (1989).
30. B. Wang, H. Liu, and G.-Y. Shi, "Radiation and cloud scheme," in *IAP Global Ocean-Atmosphere-Land System Model*, Zhang Xuehong et al., Eds., pp. 28–49, Science Press, Beijing, (2000).
31. E. J. Mlawer, S. J. Taubman, P. D. Brown, M. J. Iacono, and S. A. Clough, "Radiative transfer for inhomogeneous atmospheres: RRTM, a validated correlated-k model for the longwave," *J. Geophys. Res.* **102**, 16663–16682 (1997).
32. Z. Li, "On the solar radiation budget and the cloud absorption anomaly debate," in *Observation, Theory, and Modeling of the Atmospheric Variability*, X. Zhu, Ed., pp. 437–456, World Scientific Pub. Co., Hong Kong (2004).
33. Z. Li, L. Moreau, and A. Arking, "On solar energy disposition: a perspective from observation and modeling," *Bull. Am. Meteorol. Soc.* **78**, 53–70 (1997).
34. D. A. Randall et al., "Intercomparison and interpretation of surface energy fluxes in atmospheric general circulation models," *J. Geophys. Res.* **97**, 3711–3724 (1992).
35. Z. Li, "Intercomparison between two satellite-based products of net surface shortwave radiation," *J. Geophys. Res.* **100**, 3221–3232 (1995).
36. P. N. Francis, J. P. Taylor, P. Hignett, and A. Slingo, "On the question of enhanced absorption of solar radiation by clouds," *Q. J. R. Meteorol. Soc.* **123**, 419–434 (1997).

Hua Zhang received her BS degree in 1986 and her MS degree in 1989, both from the Nanjing Institute of Meteorology, China, and her PhD degree in 1999 from the Institute of Atmospheric Physics, Chinese Academy of Sciences, Beijing. She was an assistant researcher from April 1989 to August 1996 with the Tianjin Institute of Meteorology, China, and from September 1996 to August 2000 with the Institute of Atmospheric Physics, Chinese Academy of Sciences, Beijing. From September 2000 to July 2003, she was a postdoctoral scientist with the Institute for Global Change Research, Yokohama, Japan. Since July 2003, she has been an associate researcher with the National Climate Center, China Meteorological Administration. Dr. Zhang's specialization is radiation and she has taught atmospheric radiation at the Beijing Graduate School, China Scientific and Technological University. She has coauthored 12 papers published in technical journals and international conference proceedings.

Biographies and photographs of other authors not available.